SE-SSL-1476

SE-SSL-1476

Summary Report

CR-123636

NUCLEAR RADIATION ANALYSIS

February 1972

FEB 1972
RECEIVED
NASA STI FACILITY
INPUT BRANCH

**TELEDYNE
BROWN ENGINEERING**

Research Park • Huntsville, Alabama 35807

SUMMARY REPORT
SE-SSL-1476

NUCLEAR RADIATION ANALYSIS

By

R. J. Knies
N. R. Byrn
H. T. Smith

February 1972

Prepared for

NUCLEAR AND PLASMA PHYSICS DIVISION
SPACE SCIENCES LABORATORY
GEORGE C. MARSHALL SPACE FLIGHT CENTER

Contract No. NAS8-26557

Prepared by

SCIENCE AND ENGINEERING
TELEDYNE BROWN ENGINEERING
HUNTSVILLE, ALABAMA

ABSTRACT

This report summarizes the progress made by Teledyne Brown Engineering under Contract No. NAS8-26557. Included are descriptions of the following tasks which were accomplished:
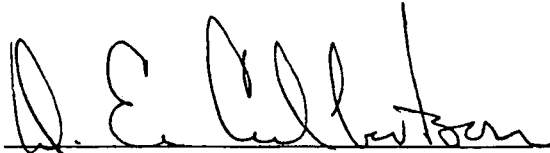
- Performed ANISN calculations of the radiation environment caused by a Bremsstrahlung photon source in a slab of aluminum

- Developed advanced techniques in Monte Carlo radiation transport calculations

- Conducted an advanced shielding class for Space Sciences Laboratory personnel to discuss theory and numerical methods for determining nuclear radiation environments

- Performed analysis of the gamma and neutron fluxes caused by cosmic-ray gamma and neutron spectra incident on a gamma-ray telescope experiment package

- Computed neutron flux and dose in a semi-infinite slab of hydrogen in water for deep penetration (100 mean free paths).

Approved: Approved:

_____   _____
N. E. Chatterton, Ph.D.   D. E. Culbertson
Manager   Vice President
Research Laboratories

TABLE OF CONTENTS

LIST OF ILLUSTRATIONS

LIST OF ILLUSTRATIONS (Concluded)

LIST OF TABLES

1. INTRODUCTION

Under Contract No. NAS8-26557, Teledyne Brown Engineering
was requested by the George C. Marshall Space Flight Center (MSFC)
to perform a study program of radiation shielding against the deleterious
effects of nuclear radiation on man and equipment. Fluxes and doses
were calculated to check out the application of the shielding programs on
the MSFC computer facility for the typical nuclear rocket shield con-
figurations and other related space apparatus. This report summarizes
the efforts to satisfy this technical directive.

Section 2 discusses the methods used to analyze the radiation
environment from Bremsstrahlung photons.

Section 3 details the various methods employed by transport
code users. The state-of-the-art capabilities and the prospective future
developments are discussed.

Section 4 outlines the steps taken during the advanced class on
radiation shielding techniques. During this seminar-workshop, the
theory and numerical methods used to solve transport of neutrons and
gammas were discussed.

Sections 5 and 6 describe the analyses of special problems. The
cosmic-ray gamma and neutron fluxes that would be present on the gamma-
ray telescope experiment were analyzed. In addition, neutron fluxes
and doses were calculated, using a slab of hydrogen in water that was
subjected to 8.1-MeV monodirectional neutrons for deep penetration
up to 100 mean free paths in the hydrogen slab. These calculations
were solved through use of the discrete ordinate S_N.

2. ANALYSIS OF THE RADIATION ENVIRONMENT CAUSED BY BREMSSTRAHLUNG PHOTONS IN A SLAB OF ALUMINUM

The Space Sciences Laboratory has been determining the Bremsstrahlung photon flux in thin materials by means of a kernel technique. Teledyne Brown Engineering personnel were requested to substantiate the kernel method by comparing the results to a transport calculation. The transport program selected was a discrete ordinates S_N program, ANISN (Ref. 2-1).

A distributed photon source spectrum as a function of energy, angle, and depth in an aluminum slab was provided by Space Sciences Laboratory. The source term data were manipulated into an acceptable format to be used in ANISN as a distributed source. A 1.85-centimeter slab of aluminum was subdivided into 42 mesh intervals, as indicated in Table 2-1. The 25-photon energy group structure with P_3 order of scattering for aluminum cross section data, as indicated in Table 2-2, was obtained from the GAMLEG-W's (Ref. 2-2) 99 fine group library at MSFC's UNIVAC-1108 tape library. ANISN was executed on the MSFC UNIVAC-1108 computer facility using an S_{16} order of angular quadrature set.

The Bremsstrahlung photon flux calculations from ANISN were forwarded to Space Sciences Laboratory personnel for comparison.

TABLE 2-1. MESH SPACING USED IN ALUMINUM SLAB FOR
BREMSSTRAHLUNG PROBLEM, 0.0- TO 1.85-cm

MESH SPACING (cm)
0.0
3.704-3*
4.7985-3
6.216-3
8.054-3
1.043-2
1.352-2
1.751-2
2.269-2
2.940-2
3.808-2
4.934-2
6.392-2
8.282-2
1.073-1
1.390-1
1.801-1
2.333-1
3.023-1
3.469-1
3.916-1
4.495-1
5.074-1
5.823-1
6.573-1
7.721-1
7.868-1
8.546-1
9.145-1
9.774-1
1.040+0
1.103+0
1.168+0
1.234+0
1.299+0
1.364+0
1.500+0
1.570+0
1.641+0
1.711+0
1.781+0
1.852+0

*Read as 3.704×10^{-3}

TABLE 2-2. PHOTON ENERGY GROUP STRUCTURE FOR
BREMSSTRAHLUNG PROBLEM

ENERGY INTERVAL (MeV)	
UPPER	LOWER
7.0	6.0
6.0	4.7
4.7	3.5
3.5	2.7
2.7	1.5
1.5	1.2
1.2	0.9
0.9	0.65
0.65	0.50
0.50	0.40
0.40	0.30
0.30	0.23
0.23	0.175
0.175	0.130
0.130	0.100
0.100	0.0750
0.0750	0.060
0.060	0.045
0.045	0.035
0.035	0.025
0.025	0.020
0.020	0.015
0.015	0.012
0.012	0.010

REFERENCES - SECTION 2

2-1. Engle, Jr., W. W., "A Users' Manual for ANISN: A One-Dimensional Discrete Ordinates Transport Code with Aniso-tropic Scattering", Report K-1693, Union Carbide Corporation, Nuclear Division, Oak Ridge Gaseous Diffusion Plant, March 30, 1970

2-2. Soltesz, R. G. and R. K. Disney, "Nuclear Rocket Shielding Methods, Modification, Updating, and Input Data Preparation", Volume 3 (U), Report No. WANL-PR-(LL)-034, Westinghouse Astronuclear Laboratory, August 1970

3. ADVANCED TECHNIQUES IN MONTE CARLO RADIATION TRANSPORT CALCULATIONS

Detailed studies were made of the dissertation, "Coupled Sampling with the Monte Carlo Method in Neutron Transport Calculations" by L. L. Carter, University of Washington (Ref. 3-1). Dr. Carter used a forward Monte Carlo calculation to determine the importance function for sampling from the adjoint equation to estimate some effect of interest, e.g., dose rate.

A continuing study of advanced techniques in Monte Carlo radiation transport calculations included the MORSE multigroup Monte Carlo code (Ref. 3-2). The MORSE code exhibits several advanced techniques that are not generally available in other Monte Carlo codes. These include simultaneous handling of neutrons, gammas, and secondary gammas by using coupled neutron-gamma cross section data and the option of solving either the forward or adjoint problem.

A recent development in the importance sampling, used by Calvin Burgart (Ref. 3-3) at Oak Ridge National Laboratory, was reviewed. Mr. Burgart used the adjoint flux from ANISN calculations as an importance function in forward Monte Carlo. Of particular interest was the selection of the direction of scattering from the altered collision kernel. Burgart's approach was to introduce an angular grid fixed in the lab system, along which particles are required to travel. This approach seems to solve the difficulties that are inherent in sampling from the collision kernel which is specified relative to the incoming particle direction.

REFERENCES - SECTION 3

3-1.   Carter, L. L., "Coupled Sampling with the Monte Carlo Method
        in Neutron Transport Calculations", University of Washington,
        Doctoral Thesis, 1969

3-2.   Straker, E. A., et al, "The MORSE Code-A Multigroup Neutron
        and Gamma-Ray Monte Carlo Transport Code", Oak Ridge
        National Laboratory, Report No. ORNL-4585, September 1970

3-3   Burgart, C. E. and P. N. Stephens, "General Method of
        Importance Sampling the Angle of Scattering in Monte Carlo
        Calculation", Oak Ridge National Laboratory, Report No.
        ORNL-TM-2890, March 1970

4. ADVANCED SHIELDING CLASS FOR SPACE SCIENCES LABORATORY PERSONNEL

An extensive seminar-workshop series was performed by Teledyne Brown Engineering for personnel of the Nuclear and Plasma Physics Division at Space Sciences Laboratory. The combination lecture and workshop was divided into the two sections listed below.

- Discussion of the development of the Boltzmann transport equation and the pertinent parameters needed by the various nuclear shielding methods

- Numerical solutions to the Boltzmann transport equations:

  ▲ Point Kernel Techniques using the KAP-VI computer program

  ▲ Discrete Ordinates S_N techniques using the DOT-IIW computer program

  ▲ Monte Carlo Techniques using the CAVEAT computer program.

4.1   DEVELOPMENT OF BOLTZMANN TRANSPORT EQUATION

The development of the Boltzmann transport equation was derived from the physical phenomonology of a particle balance. The technique of reducing the Boltzmann transport equation to a form amenable to solution was demonstrated by the use of the spherical harmonics, and the P_1 approximation to give the transport corrected diffusion equation. Also included in the presentation was an explanation concerning the mathematical and physical concepts of quantities such as particle density, flux, fluence, and current that are used to describe radiation fields.

4-1

4.2 NUMERICAL SOLUTION TO BOLTZMANN TRANSPORT EQUATION

The numerical methods for solution of the transport equation discussed by Teledyne Brown Engineering were the Point Kernel KAP-VI (Ref. 4-1), Discrete Ordinate DOT-IIW (Ref. 4-2), and Monte Carlo CAVEAT Programs (Ref. 4-3).

For all three numerical methods, a general geometric model of the nuclear rocket reactor and attached propellant tank configuration was used. The model is shown in Figures 4-1 and 4-2.

4.2.1 Discussion of Seminar-Workshop on the Use of KAP-VI

The development, use, accuracy, and limitations of the Point Kernel calculation techniques were discussed during the presentation of the theory. KAP-VI as a point kernel transport code involves the representation of a source by a number of point isotropic sources and computes the attenuation along a ray through all geometric regions traversed by the line-of-sight method to the receiver point.

Following the general treatment of the KAP-VI theory, an extensive study was made of the KAP-VI input data. During the workshop phase of the course, emphasis was given to a detailed explanation of each piece of KAP-VI input data necessary to compute the radiation environment. This explanation gave the reasons why the particular data was used and identified the source of data to be used in solving other KAP-VI problems.

KAP-VI data can be categorized in the following areas:

- Neutron and gamma source radial and axial mesh distributions. A distribution for workshop problems is shown in Figures 4-3 and 4-4.
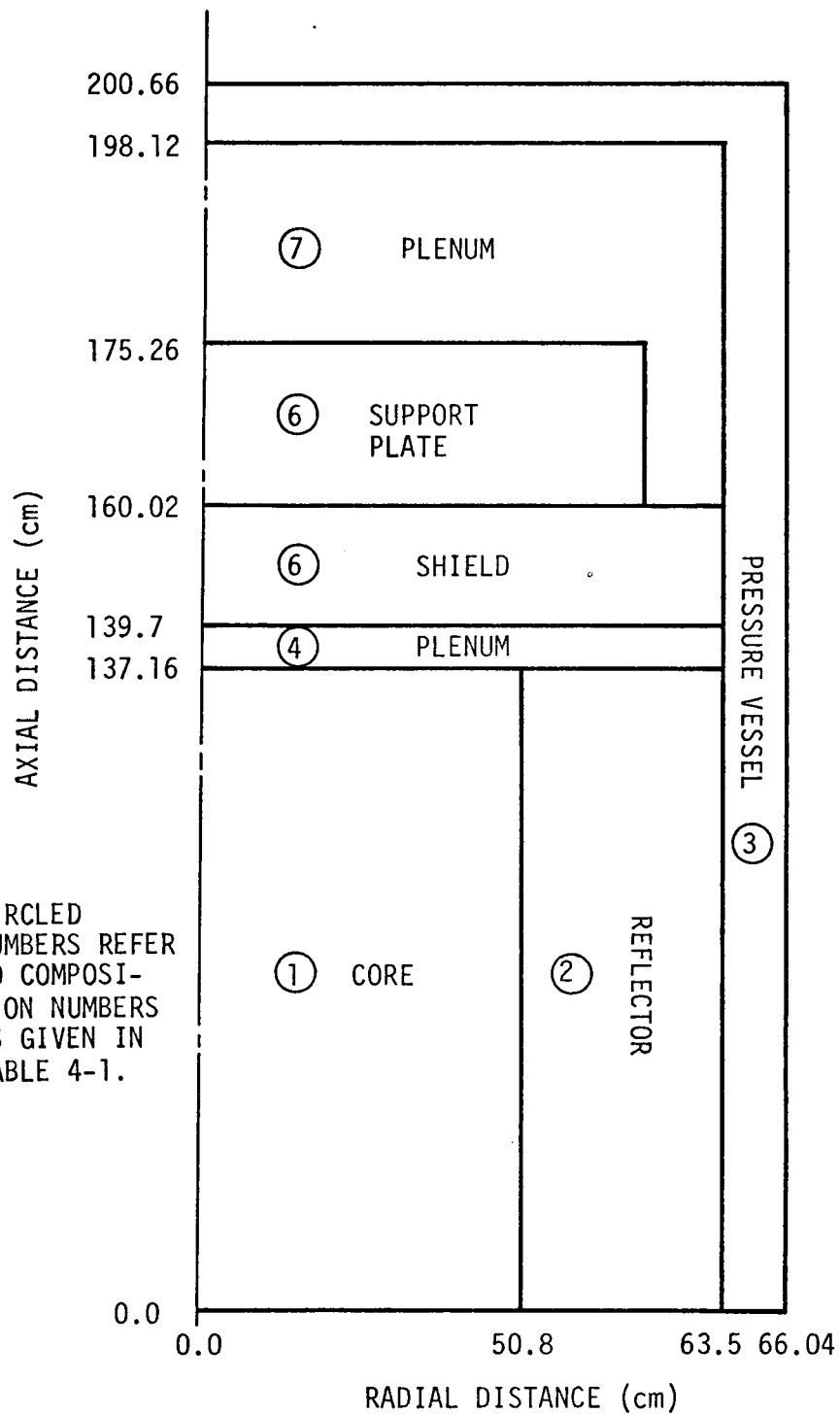
FIGURE 4-1. BASIC REACTOR GEOMETRY FOR THE SAMPLE PROBLEM
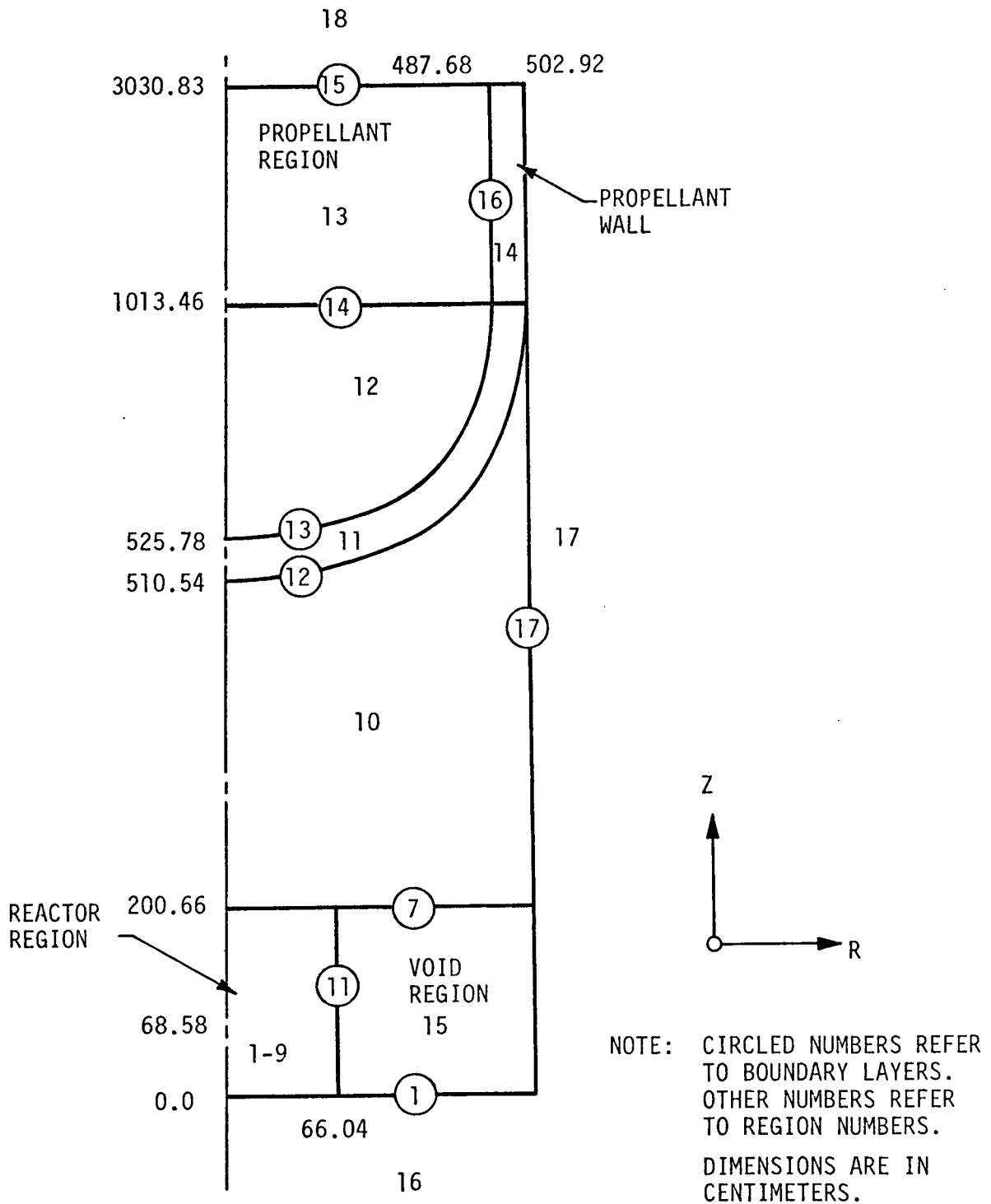
FIGURE 4-2. GEOMETRICAL MODEL FOR THE REACTOR AND PROPELLANT TANK CONFIGURATION
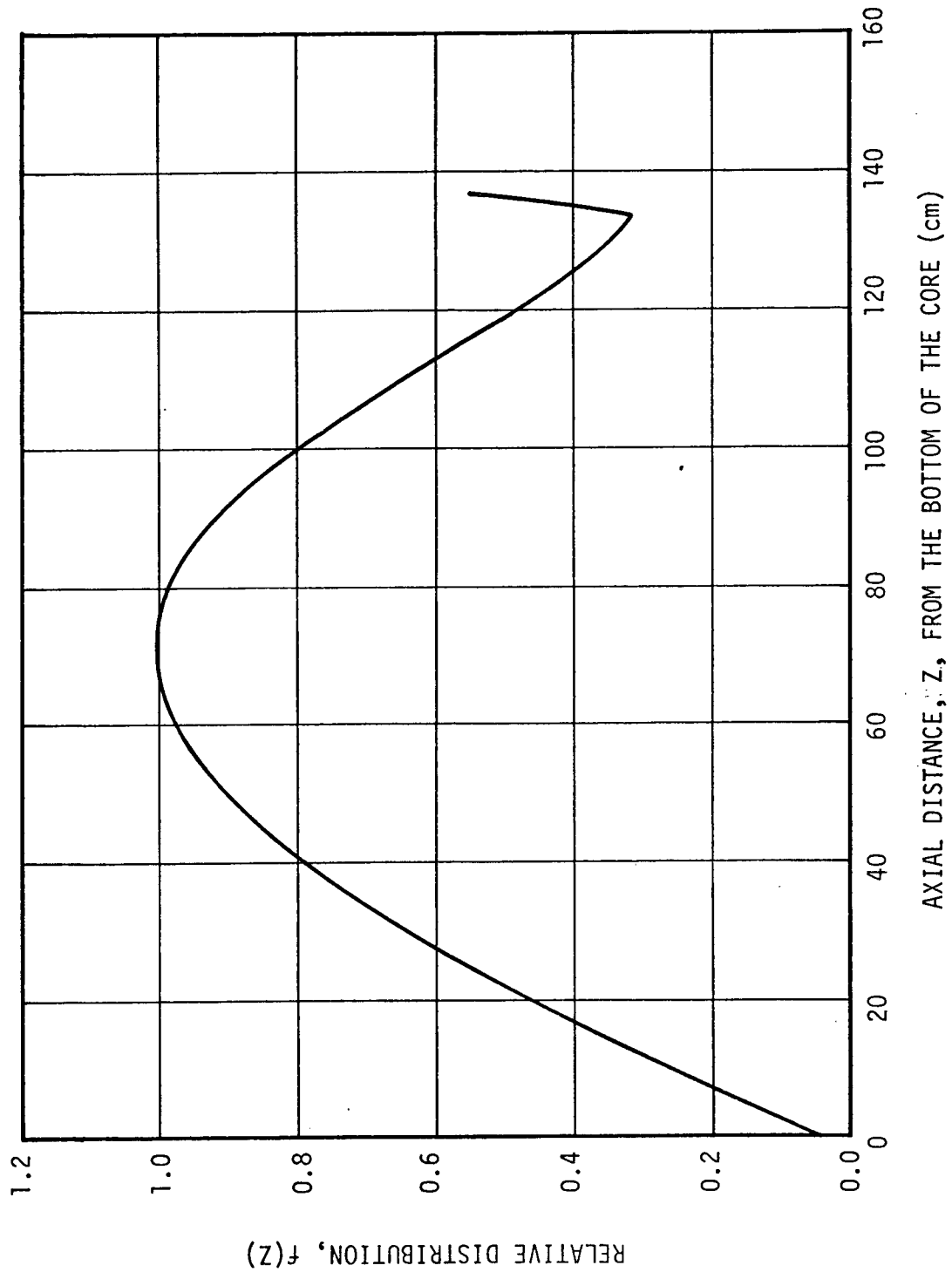
FIGURE 4-3. RELATIVE AXIAL DISTRIBUTION OF THE FISSION SOURCE IN THE REACTOR
CORE - REGION 1
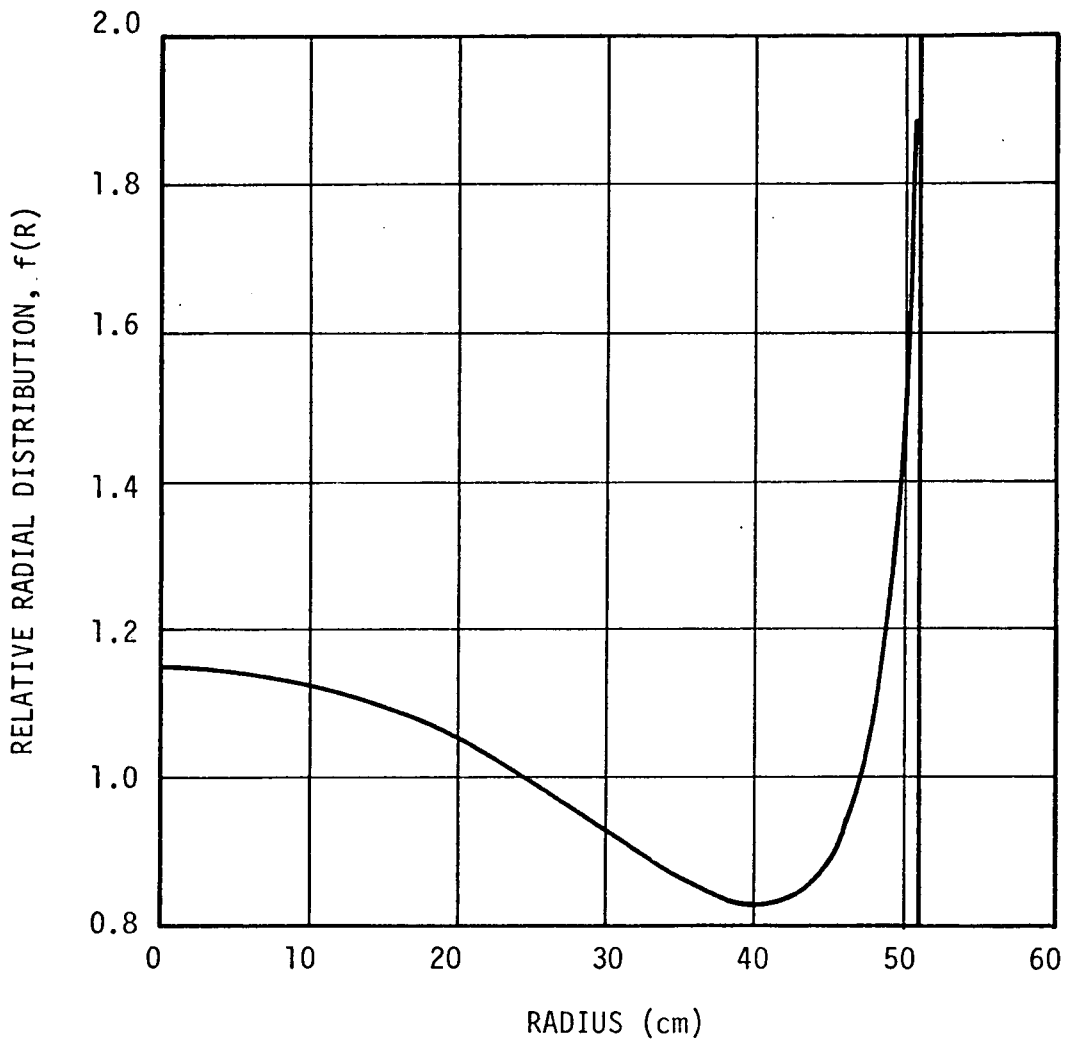
FIGURE 4-4.   RELATIVE RADIAL DISTRIBUTION OF THE SOURCE
IN THE REACTOR CORE - REGION 1

- Geometry of a system as a group of zones and boundary surfaces

- Material composition matrix. A matrix used in the workshop is shown in Table 4-1.

- Neutron and gamma energy or particle spectra data

- Energy group dependent response data to convert particle flux or energy flux to dose and/or heating rates

- Fast neutron removal cross section data

- Gamma mass absorption attenuation coefficients

- Gamma buildup coefficient data

- Neutron bivariant or monovariant spectra polynomial data.

During the workshop an explanation of the KAP-VI data entries and the source of the data in the available reference material was given. The input data instructions were placed on computer data forms by the participants during the workshop sessions. Several KAP-VI data decks for the nuclear rocket reactor model were submitted for execution on the MSFC UNIVAC 1108 computer. The KAP-VI nuclear rocket neutron and gamma output at selected points was discussed. Continuing effort and periodic technical assistance with Space Sciences Laboratory personnel have been directed for similar KAP-VI problems associated with NASA efforts. Recently, effort was focused on a SNAP power generator model for a neutron and gamma analysis using KAP-VI.

4.2.2 Discussion of Seminar-Workshop on the use of DOT-IIW

Several lecture sessions were devoted to the theory of the discrete ordinates solution to the Boltzmann transport equation and in the instructions in the practical use of a discrete ordinates S_N program.

TABLE 4-1. MATERIAL COMPOSITIONS FOR KAP-VI

COMP. NO* AND DESCRIPTION	MATERIAL										
	H	Be	B	C	N	Al	Cr	Fe	Ni	Nb	U
1 Core	5.36(-4)**	---	---	1.504(0)	---	---	3.89(-4)	2.67(-3)	5.27(-3)	3.08(-3)	7.31(-2)
2 Reflector	1.40(-3)	1.656(0)	---	---	---	---	---	---	---	---	---
3 Pressure Vessel	---	---	---	---	---	2.8(0)	---	---	---	---	---
4 Plenum	6.3(-2)	---	---	---	---	---	---	---	---	---	---
5 Shield	4.73(-2)	---	1.98(-2)	---	---	---	3.76(-1)	1.416(0)	1.88(-1)	---	---
6 Support Plate	1.26(-2)	---	---	---	---	2.24(0)	---	---	---	---	---
7 "Void"	---	---	---	---	1.0(-8)	---	---	---	---	---	---
8 Tank Wall	---	---	---	---	---	8.4(-2)	---	---	---	---	---
9 Propellant	7.0(-2)	---	---	---	---	---	---	---	---	---	---

*The composition number to be associated with regions shown in Figures 4-1 and 4-2.
**Read as 5.36×10^{-4}.

The two-dimensional, time-independent, discrete ordinates program, DOT-IIW, was used to determine the neutron flux and/or dose for the nuclear reactor assembly. The neutron flux and dose were determined for the R-Z geometry described in Figure 4-1. A neutron distributed source in the R and Z mesh intervals of the reactor core region was established in accordance with data obtained from Figures 4-3 and 4-4.

The neutron cross section for the elements in the reactor region were assembled from a Westinghouse elemental cross section library. The cross section set considers an energy group structure with 16 energy intervals as tabulated in Table 4-2, and with P_0 order of scatter for the elements, as listed in Table 4-2. An S_2 quadrature set was used in the solution, employing a mesh spacing of 32 radial and 36 axial intervals for the complete system description.

In the workshop session, a step-by-step explanation of each data entry was given. Interpretations of the results from DOT-IIW were discussed with the members attending the seminar-workshop.

4.2.3 Discussion of Seminar-Workshop on the use of CAVEAT

The Monte Carlo program CAVEAT was used to determine the gamma fluxes and doses for the nuclear rocket reactor geometry model, as shown in Figure 4-1. The gamma source distribution in the reactor core region was subdivided into intervals on the R and Z axis, based on data obtained from Figures 4-3 and 4-4.

The gamma point cross section data were obtained from data tabulated by Storm and Israel (Ref. 4-4) for elements shown in Table 4-1.

In the workshop session, each data entry was thoroughly explained. An analysis of the dose and flux results from CAVEAT was discussed by the members attending the seminar-workshop.

TABLE 4-2. DOT-IIW NEUTRON ENERGY GROUP STRUCTURE AND ELEMENT
LIST FOR NUCLEAR ROCKET SEMINAR-WORKSHOP

ELEMENT GROUP	ENERGY INTERVAL BOUNDS (eV)	ELEMENT LIST
1	2.87×10^6 to 1.0×10^7	
2	1.35×10^6 to 2.87×10^6	H
3	8.21×10^5 to 1.35×10^6	Be
4	3.88×10^5 to 8.21×10^5	B
5	1.11×10^5 to 3.88×10^5	C
6	1.50×10^4 to 1.11×10^5	Al
7	5.53×10^3 to 1.50×10^4	Cr
8	5.83×10^2 to 5.53×10^3	Fe
9	7.89×10^1 to 5.83×10^2	Ni
10	1.07×10^1 to 7.89×10^1	Nb
11	1.86×10^0 to 1.07×10^1	U-235
12	3.0×10^{-1} to 1.86×10^0	U-238
13	1.2×10^{-1} to 3.0×10^{-1}	
14	6.0×10^{-2} to 1.2×10^{-1}	
15	2.0×10^{-2} to 6.0×10^{-2}	
16	0.0 to 2.0×10^{-2}	

REFERENCES - SECTION 4

4-1.   Disney, R. K. and S. L. Zeigler, "Nuclear Rocket Shielding
        Methods, Modification, Updating, and Input Data Preparation",
        Volume 6 (U), Westinghouse Astronuclear Laboratory, Report
        No. WANL-PR-(LL)-034, August 1970

4-2.   Soltesz, R. G. and R. K. Disney, "Nuclear Rocket Shielding
        Methods, Modification, Updating, and Input Data Preparation",
        Volume 5 (U), Westinghouse Astronuclear Laboratory, Report
        No. WANL-PR-(LL)-034, August 1970

4-3.   Byrn, N. R., "CAVEAT: A Revised Version of the General
        Purpose Monte Carlo Program, COHORT, Volumes I and II
        (U)", Teledyne Brown Engineering Technical Note SE-290,
        October 1969

4-4.   Storm E. and H. I. Israel, "Photon Cross Sections from 0.001
        to 100 MeV for Elements 1 through 100", Los Alamos Scientific
        Laboratory, Report No. LA-3753, June 1967

5. GAMMA-RAY TELESCOPE RADIATION ENVIRONMENT

Calculations were made of the neutron and gamma-ray flux in the NaI detector of the gamma-ray telescope caused by the cosmic-ray neutron and gamma spectrum expected to be incident on the telescope assembly when in operation. The two-dimensional discrete ordinates code, DOT (Ref. 4-2), was used to perform the calculations. The discrete ordinates methods of solving the transport equation is based on the iterative solution of the transport equation written in finite difference form. Neutron and gamma-ray cross sections were represented in multigroup form and treated anisotropic scattering with a P_1 order of Legendre expansion; an S_8 order of angular quadrature was used, which means that 48 spatial angles were considered in calculating the angular and scalar flux at each point.

A boundary source condition was applied to all sides of the telescope assembly to represent the neutron and gamma flux which would be experienced in actual operation. The flux was assumed to be isotropic, the actual values of flux that were used in the calculation are shown in Figures 5-1, 5-2, and 5-3. A check with the boundary replaced by a void, i.e., there was no material present in the calculation, reproduced the incident fluxes (Figures 5-1, 5-2, and 5-3) at all locations within the void region. This apparent trivial calculation is quite important, in that any of the most commonly made errors in setting up a problem of this type are made obvious as a result.

The actual geometry of the experiment package is shown in Figure 5-4. As recommended, the photomultiplier tubes and the 3/8-inch thick aluminum base plate were not considered in the calculation. Using the R-Z geometry option in DOT, a mockup of the telescope

FIGURE 5-1.   ATMOSPHERIC GAMMA-RAY SPECTRUM
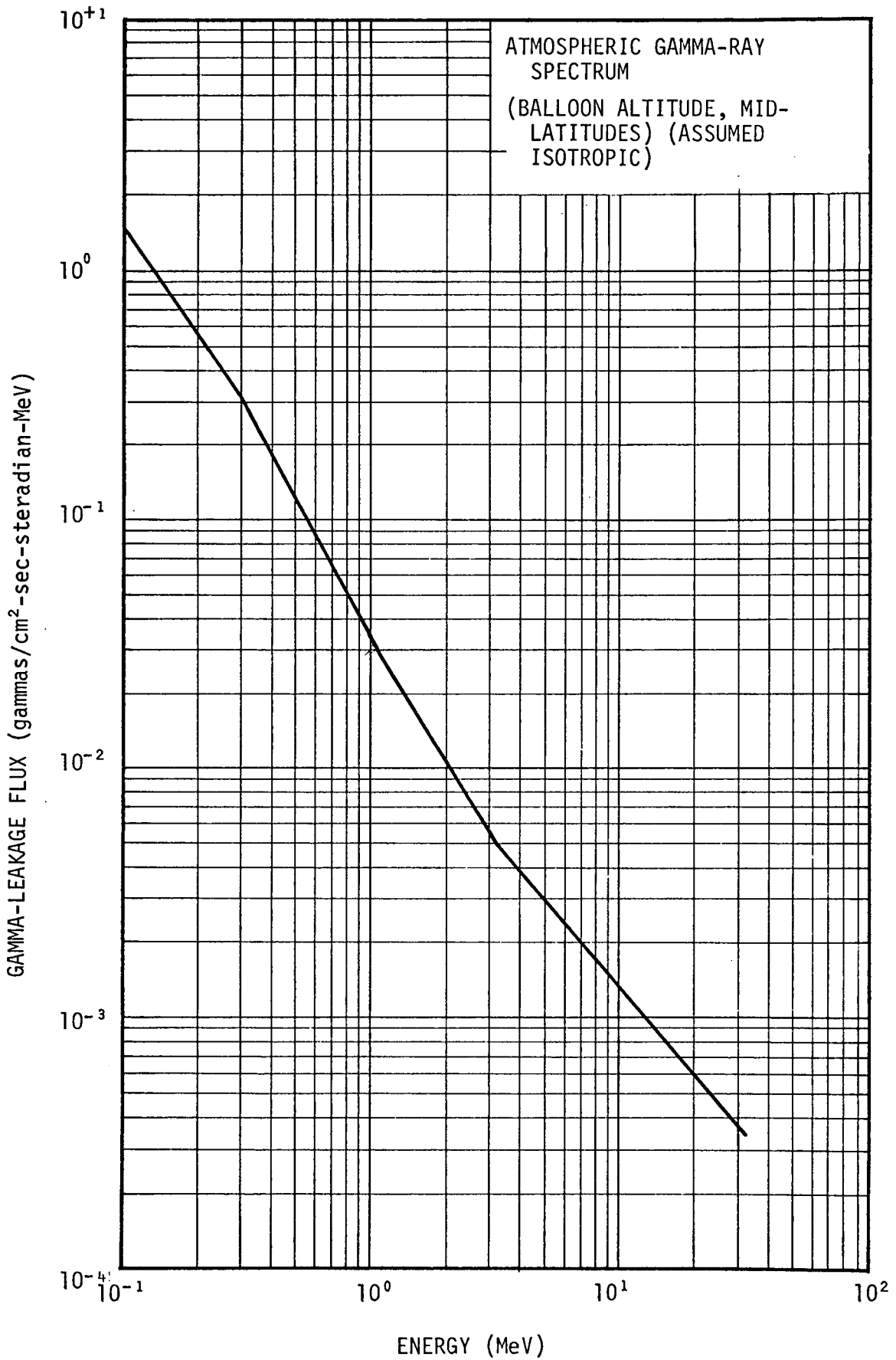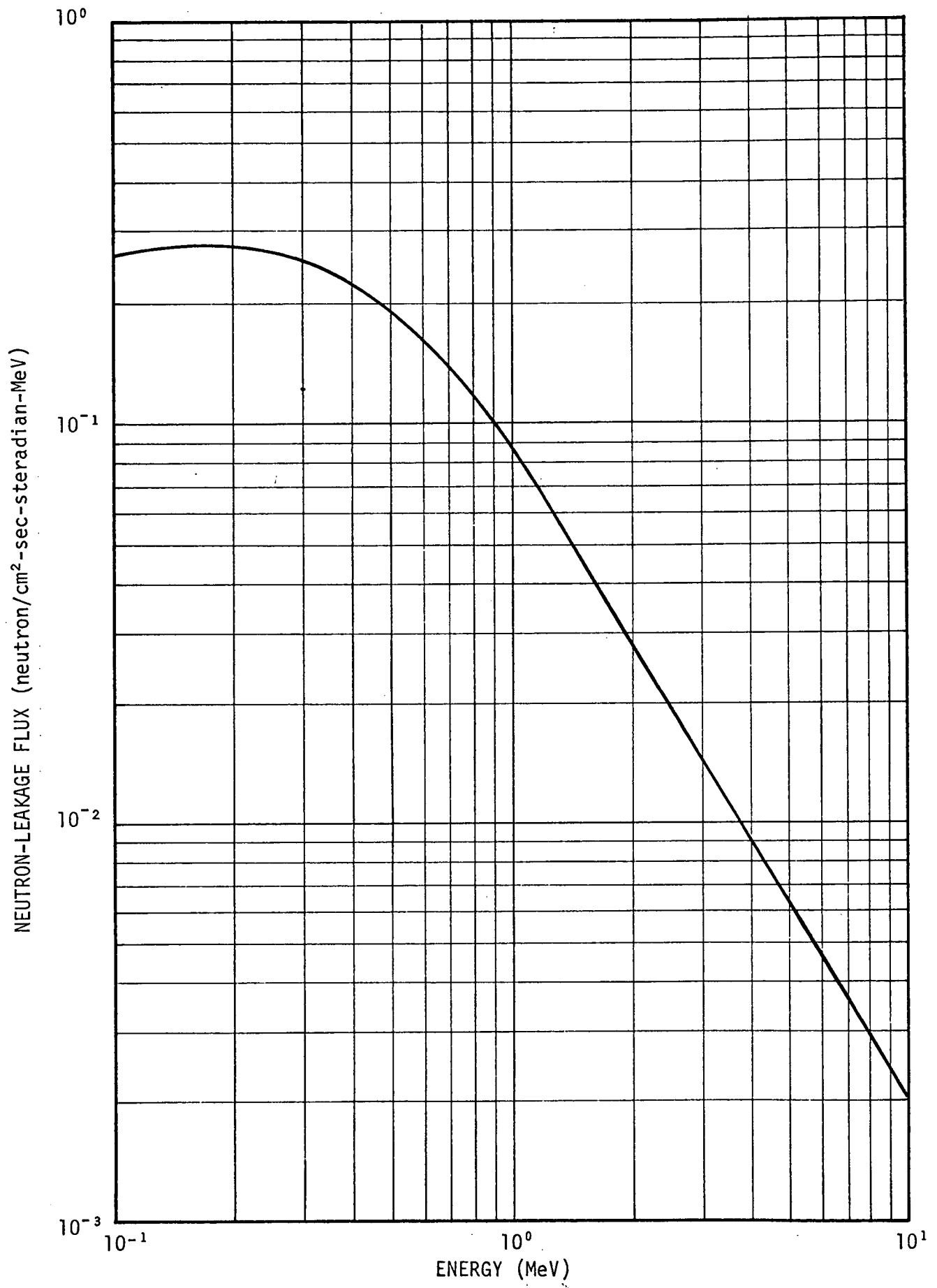
FIGURE 5-2. ATMOSPHERIC NEUTRON SPECTRUM BALLOON ALTITUDE,
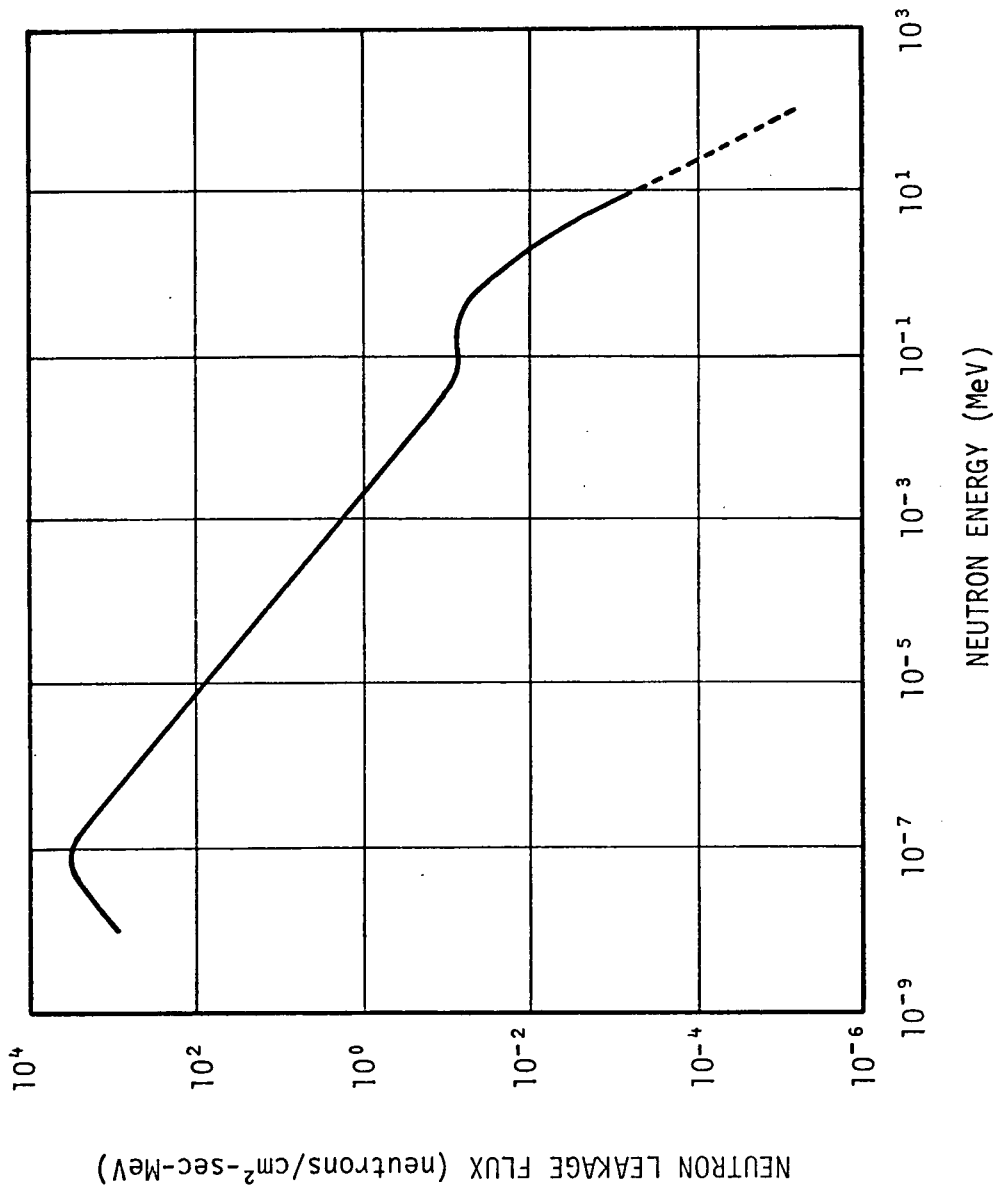   MID-LATITUDE

5-3

FIGURE 5-3. COSMIC-RAY NEUTRON LEAKAGE FLUX SPECTRUM AT 0-DEGREE GEOMAG-
NETIC LATITUDE FOR SOLAR MINIMUM (1953-54) (Graph reprint from
Lingenfelter, R.E., "Cosmic-Ray Neutron Leakage Flux", Journal
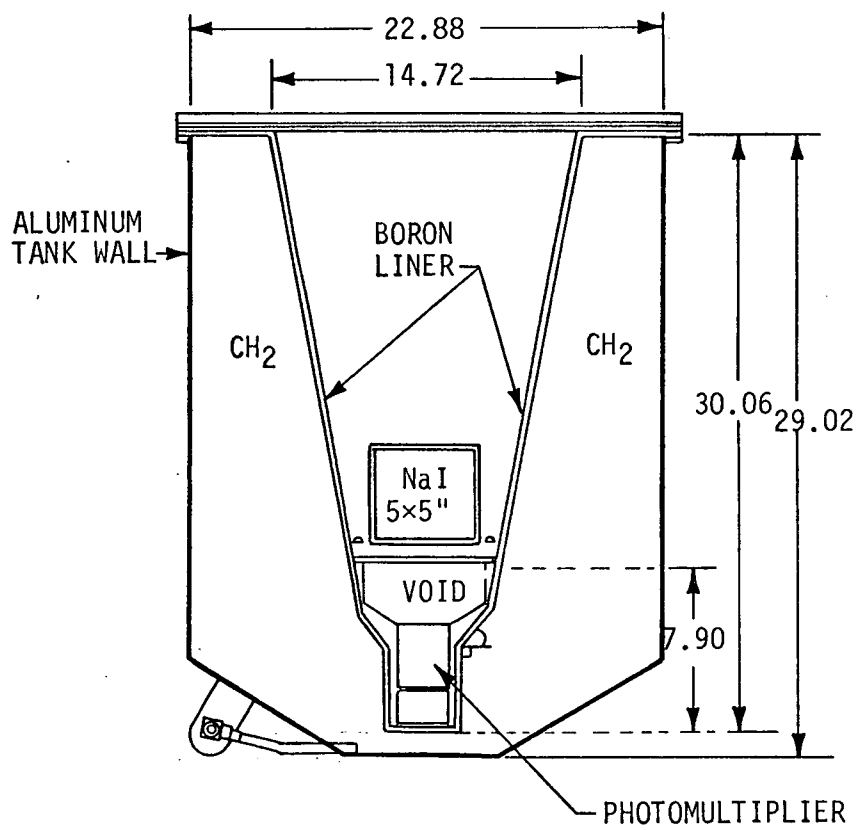of Geophysical Research, Vol. 68, No. 20, October 1963)

FIGURE 5-4. GAMMA-RAY TELESCOPE GEOMETRY

assembly was made, as shown in Figure 5-5. Note that surfaces and zone boundaries used in DOT must be either constant z radial planes, or cylindrical surfaces of constant radius from the center line (therefore conical regions), such as the boron liner on the inner wall of the mineral oil container which must be represented by a series of concentric cylindrical annuli. There is a commonly used method of mocking up conical regions with cylindrical geometry which is quite reliable, provided the total amount of material is the same in both cases and provided there are not significant "windows" remaining in the material where streaming of radiation could occur. Care was taken in meeting both of these conditions. A similar representation was made of the region which contains the NaI scraps in mineral oil.

A 47-group energy structure was used for the calculation, comprised of 27 neutron energy groups and 20 gamma groups; Table 5-1 lists the upper boundaries of these groups. Microscopic cross sections were obtained from the Oak Ridge National Laboratory in this 47-group structure, for all elements that were present in the geometry. The microscopic cross sections were multiplied by the elemental number densities to obtain a set of macroscopic cross sections for each region in the problem. Normally, microscopic cross sections are input into DOT along with the number densities for each element in a material, and the code then calculates its own macroscopic cross sections. However, in this case, the cross section "mixing" was done with a separate code before running DOT to make more computer core storage locations available for the transport calculation. In this case, there was still a severe limitation on the problem size using MSFC's UNIVAC 1108 system, and the calculation, as described, was the most detailed representation of the actual problem that could be run. Because of the method of
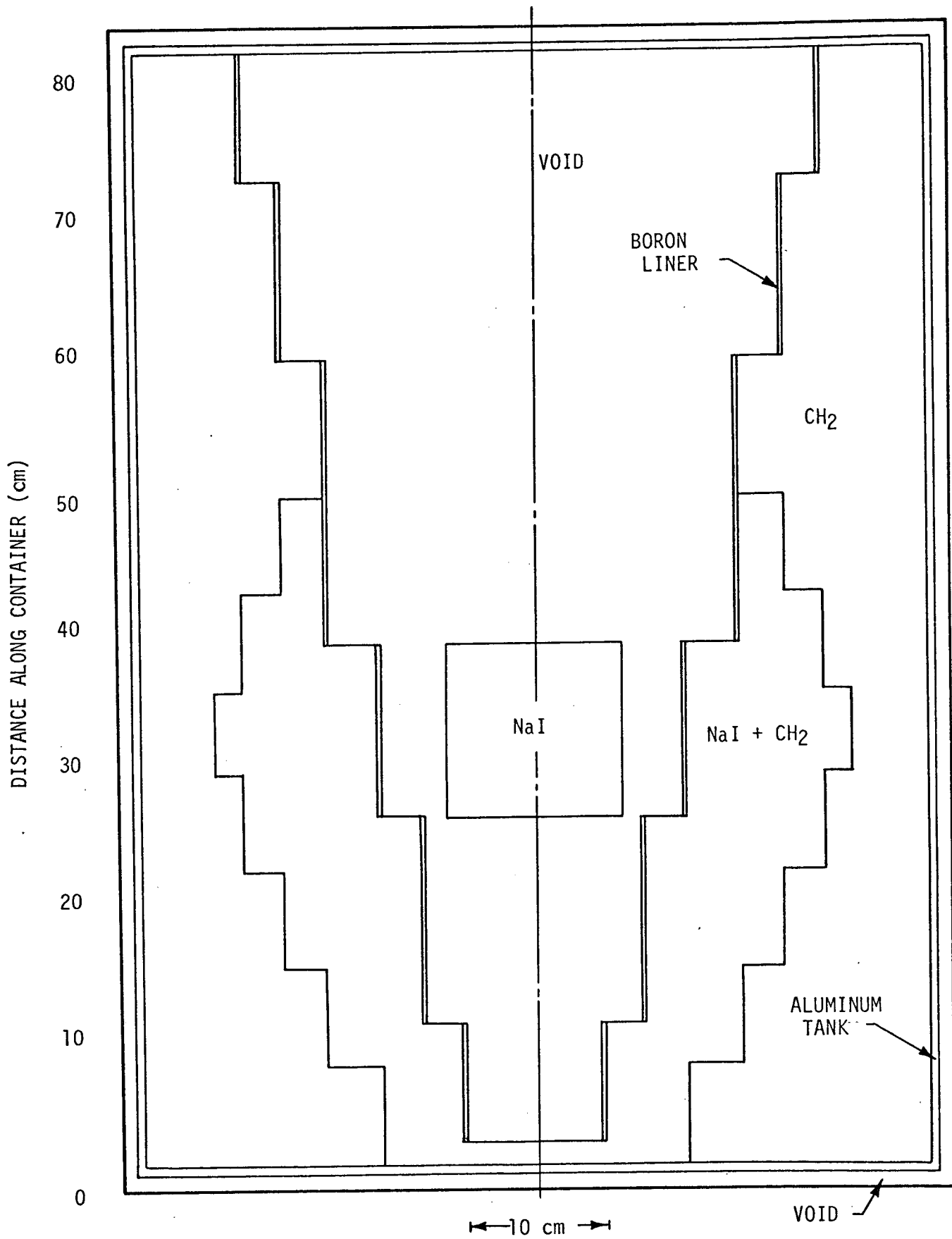
FIGURE 5-5. DOT CALCULATIONAL GEOMETRY

5-7

TABLE 5-1. UPPER BOUNDARIES OF A 47-GROUP ENERGY STRUCTURE

NEUTRON		PHOTON	
GROUP	UPPER ENERGY BOUNDS (eV)	GROUP	UPPER ENERGY BOUNDS (eV)
1	1.49 (+7)*	1	1.0 (+7)
2	1.22 (+7)	2	8.0 (+6)
3	1.00 (+7)	3	7.0 (+6)
4	8.19 (+6)	4	6.0 (+6)
5	6.70 (+6)	5	5.0 (+6)
6	5.49 (+6)	6	4.0 (+6)
7	4.49 (+6)	7	3.5 (+6)
8	3.67 (+6)	8	3.0 (+6)
9	3.01 (+6)	9	2.5 (+6)
10	2.47 (+6)	10	2.0 (+6)
11	2.02 (+6)	11	1.6 (+6)
12	1.65 (+6)	12	1.2 (+6)
13	1.35 (+6)	13	9.0 (+5)
14	1.10 (+6)	14	6.0 (+5)
15	9.07 (+5)	15	4.0 (+5)
16	6.08 (+5)	16	3.0 (+5)
17	4.08 (+5)	17	2.1 (+5)
18	1.11 (+5)	18	1.6 (+5)
19	1.50 (+4)	19	1.2 (+5)
20	3.35 (+3)	20	7.0 (+4) -
21	5.83 (+2)		1.0 (+4)
22	1.01 (+2)		
23	2.90 (+1)		
24	1.07 (+1)		
25	3.06 (+0)		
26	1.13 (+0)		
27	4.14 (-1) -		
	2.50 (-2)		

*Read as 1.49×10^7

solution in discrete ordinate programs, it is not possible to have a boundary source incident on all sides of the geometry at once, therefore the calculation was made twice, once with the source on the top and sides, and secondly with the source on the bottom. To determine the total flux, the results of these calculations were then added. The fluxes were calculated at 12 points within the NaI crystal. A linear average of the four points on the center plane of the crystal was made and that is the value shown in the results.

The final results are listed in Table 5-2, and are shown in Figures 5-6 through 5-9, as differential number flux (neutrons or gammas/cm^2-sec-energy group width). As mentioned previously, this is the flux at the center of the NaI detector. But, if there are any other locations at which the flux is desired, they are presently available in a similar manner, since the discrete ordinates method of solution provides results at all mesh points in the geometry (there were 380 mesh points in this problem) for each calculation.

TABLE 5-2. DIFFERENTIAL NUMBER FLUX USING A 47-GROUP ENERGY STRUCTURE

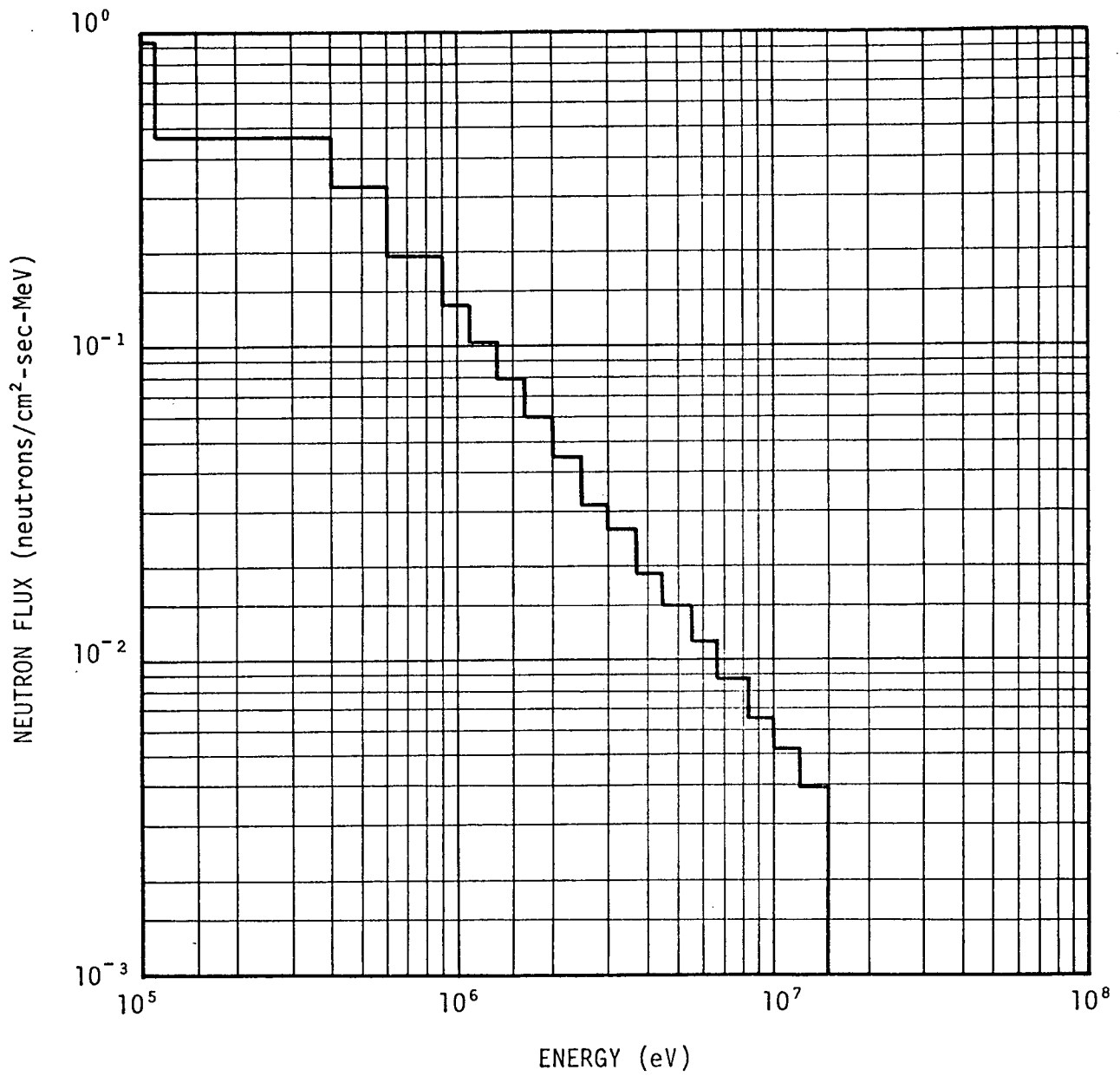| GROUP	NEUTRON DIFFERENTIAL NUMBER FLUX (neutrons/cm^2-sec-MeV)	GROUP	PHOTON DIFFERENTIAL NUMBER FLUX (photons/cm^2-sec-MeV)
1	3.92 (-3)*	1	4.09 (-3)
2	5.19 (-3)	2	5.62 (-3)
3	6.56 (-3)	3	2.44 (-2)
4	8.76 (-3)	4	2.70 (-2)
5	1.14 (-2)	5	8.76 (-2)
6	1.49 (-2)	6	9.52 (-2)
7	1.87 (-2)	7	1.02 (-1)
8	2.64 (-2)	8	1.94 (-1)
9	3.21 (-2)	9	2.22 (-1)
10	4.43 (-2)	10	1.43 (-1)
11	5.98 (-2)	11	1.79 (-1)
12	7.88 (-2)	1	2.41 (-1)
13	1.03 (-1)	13	3.63 (-1)
14	1.35 (-1)	14	1.28 (0)
15	1.92 (-1)	15	9.40 (-1)
16	3.25 (-1)	16	8.34 (-1)
17	4.65 (-1)	17	5.72 (-1)
18	9.24 (-1)	18	2.02 (-1)
19	2.98 (0)	19	2.72 (-2)
20	1.46 (+1)	20	8.23 (-2)
21	6.77 (+1)		
22	1.92 (+2)		
23	7.25 (+2)		
24	1.73 (+3)		
25	3.20 (+3)		
26	5.38 (+3)		
27	6.84 (+4)		

*Read as 3.92 × 10^{-3}

FIGURE 5-6. NEUTRON FLUX AS A FUNCTION OF ENERGY IN
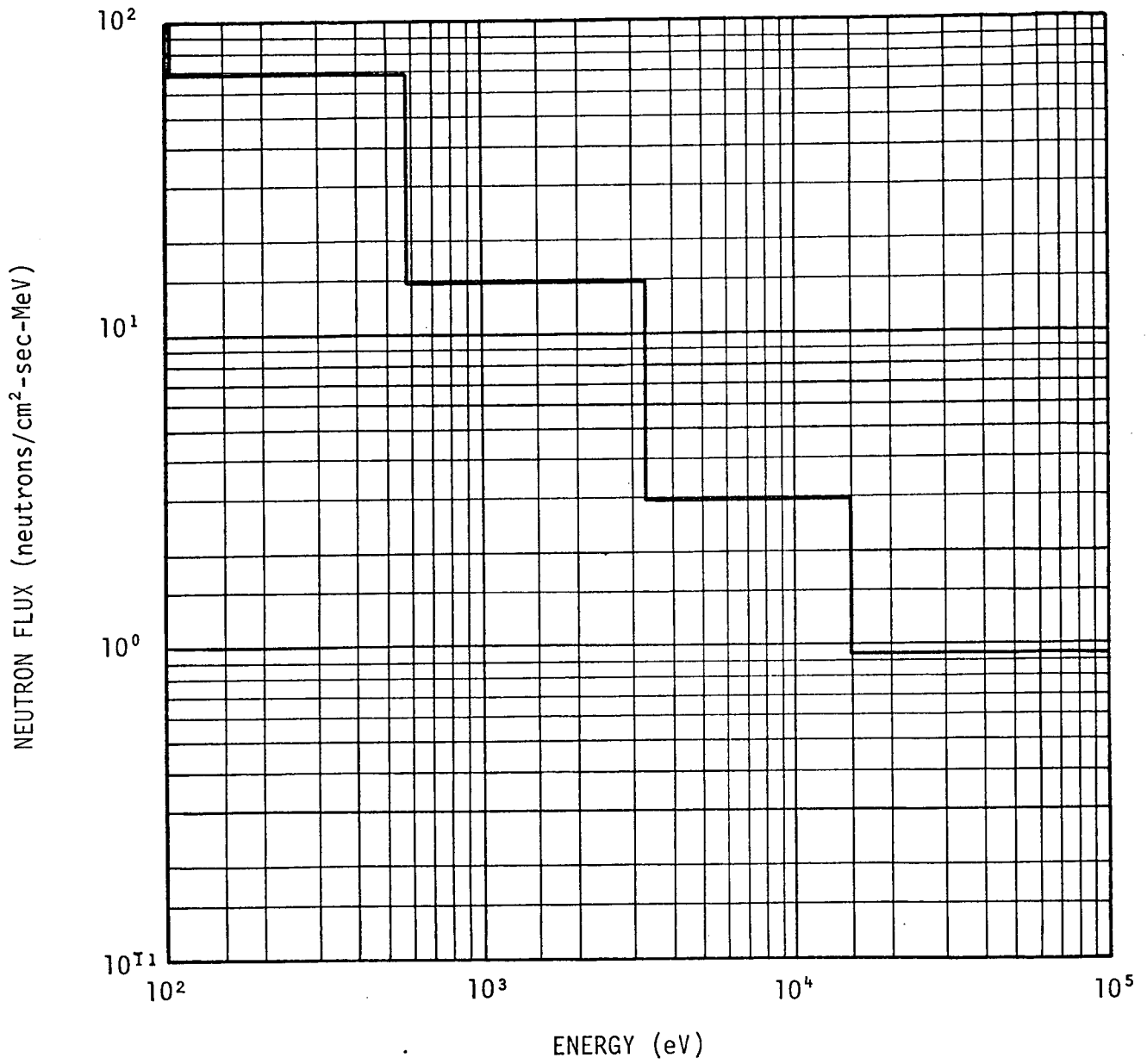NaI DETECTOR (10^8 TO 10^5 eV)

FIGURE 5-7.   NEUTRON FLUX AS A FUNCTION OF ENERGY IN
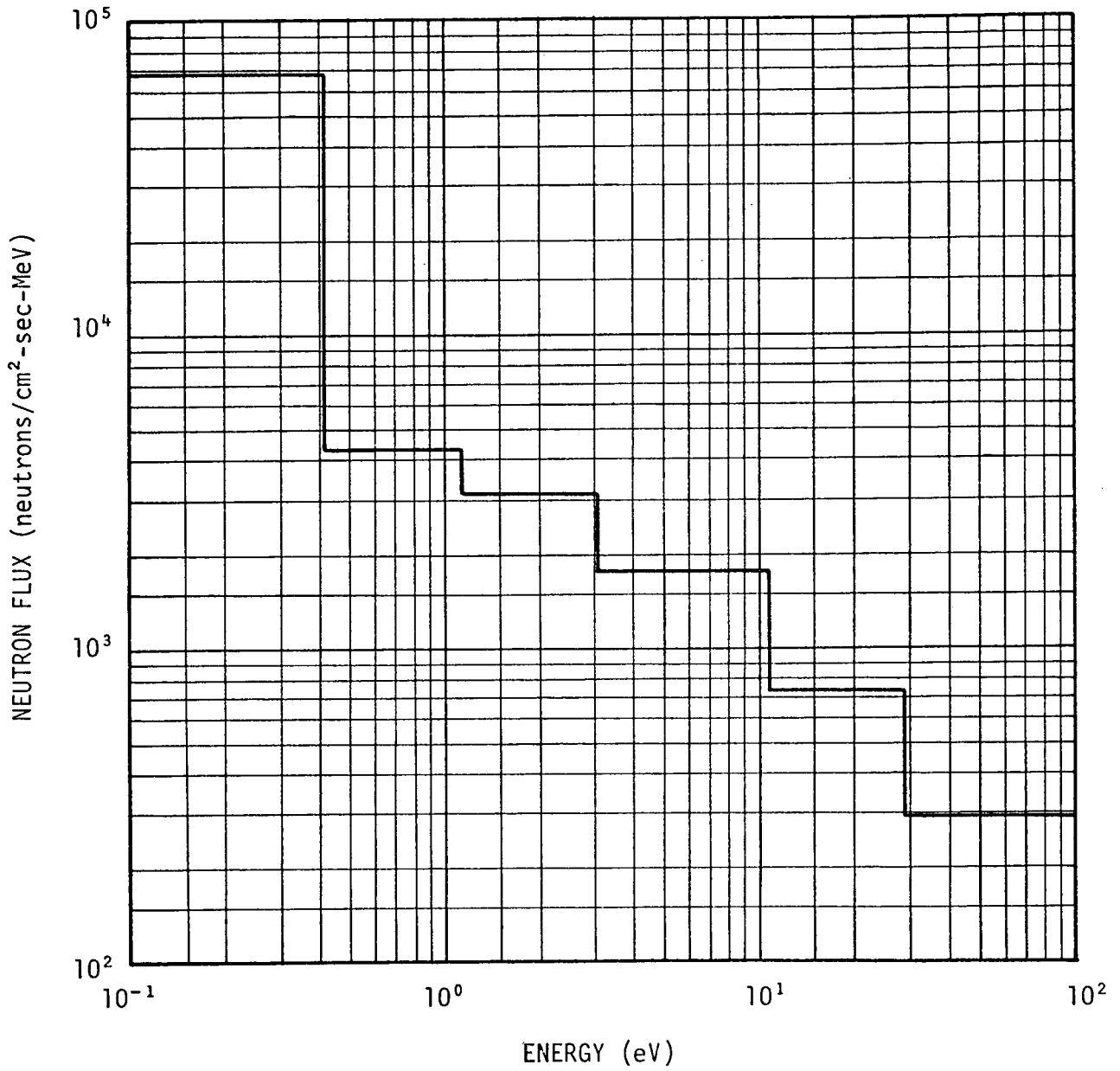   NaI DETECTOR (10^5 TO 10^2 eV)

FIGURE 5-8.   NEUTRON FLUX AS A FUNCTION OF ENERGY IN
              NaI DETECTOR (10^2 TO 10^{-1} eV)
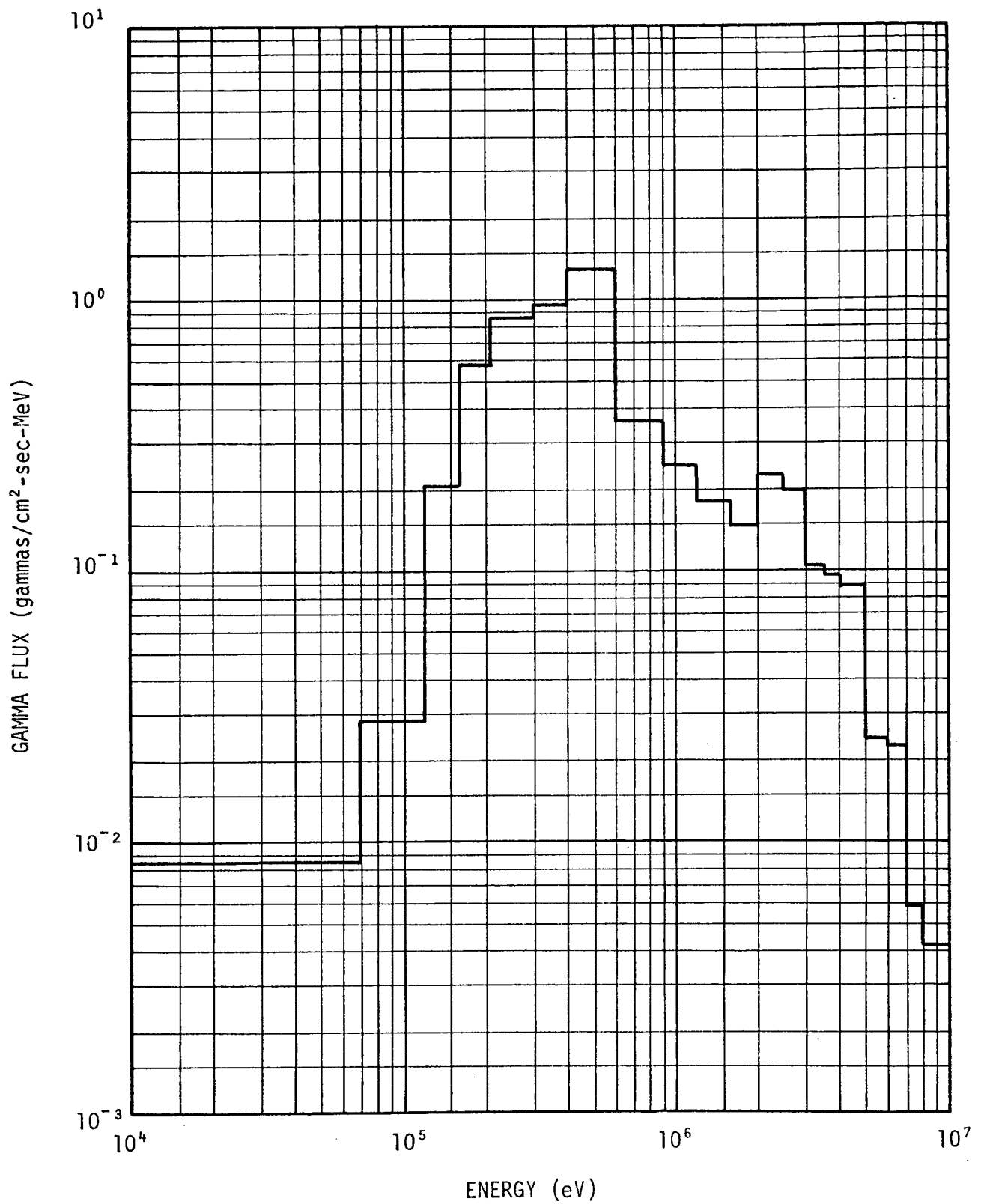
FIGURE 5-9.   GAMMA FLUX AS A FUNCTION OF ENERGY IN
NaI DETECTOR

5-14

6. NEUTRON PENETRATION THROUGH A SLAB OF HYDROGEN USING DISCRETE ORDINATES TECHNIQUES

In previous analyses of neutron penetration through thick hydrogen slabs, Monte Carlo techniques employing importance sampling methods (Ref. 6-1) have been used to improve accuracy. In deep penetration the Monte Carlo process requires both a considerable amount of computer time and insight relative to choosing the proper importance function for the sampling schemes. As a comparison on computer time and accuracy of results, the discrete ordinate program ANISN (Ref. 6-2) was employed to calculate the neutron flux, single collision doses, and multicollision doses through semi-infinite slabs of hydrogen. These calculations can be used to determine the fast dose buildup factors at values up to 100 mean free paths.

6.1 MODELS AND METHODS USED IN TRANSPORTING NEUTRONS IN HYDROGEN

To determine the neutron flux and doses from a beam of 8.1-MeV neutrons that is normally incident on a semi-infinite slab of hydrogen in water, the one-dimensional ANISN discrete ordinate S_N program was used. The model that was used to simulate the conditions consisted of a semi-infinite slab of hydrogen having a density of 0.111 g/cm^3, which corresponds to the hydrogen density in water. A diagram of the geometric mesh spacing employed in ANISN is given in Figure 6-1. The one-dimensional slab geometry was used with vacuum interfaces on the left and right boundaries. The mesh spacing was selected with a fine mesh near the boundaries and a course mesh in the center. The course mesh spacing was varied from approximately 0.125 to 1.0 mean free path for a neutron energy group of 7 to 8 MeV. Evaluation of flux and dose was not allowed near the vacuum boundaries, since end effects

in ANISN would distort the results. Location of the source was in the first mesh cell, as shown in Figure 6-2. The first mesh cell has an overall dimension of less than 1 centimeter.
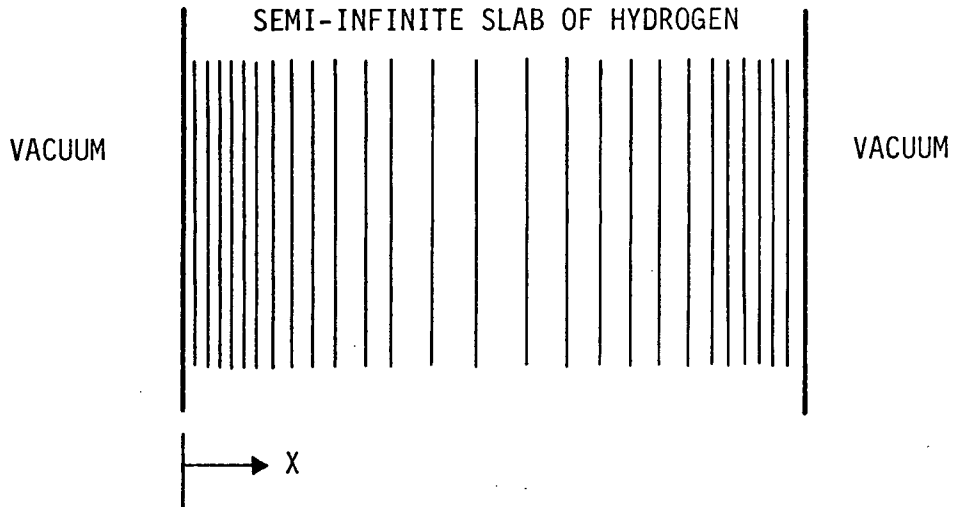
FIGURE 6-1. MESH SPACING FOR A SLAB OF HYDROGEN IN WATER, USING ANISN

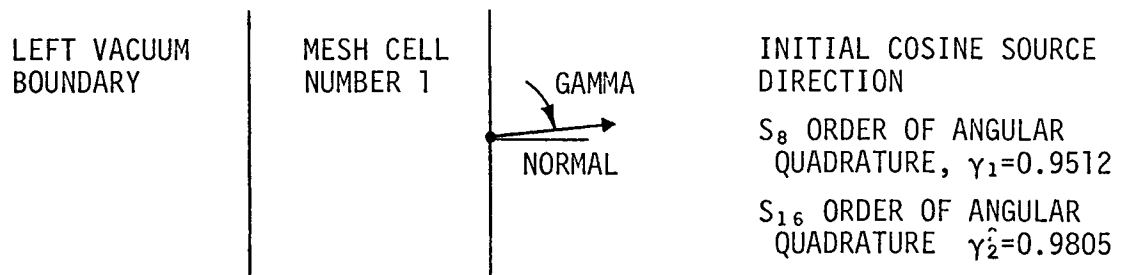| LEFT VACUUM BOUNDARY	MESH CELL NUMBER 1	GAMMA NORMAL	INITIAL COSINE SOURCE DIRECTION
			S_8 ORDER OF ANGULAR QUADRATURE, $\gamma_1 = 0.9512$
			S_{16} ORDER OF ANGULAR QUADRATURE $\gamma_2^{\circ} = 0.9805$

FIGURE 6-2. SOURCE REGION DESCRIPTION

In ANISN, the shell source method was used. This method places the source on the right boundary surface of the first mesh cell. The energy group structure that was used is shown in Table 6-1. The P_3 hydrogen-neutron cross section data corresponding to this energy group structure were obtained from the Radiation Shielding Information Center (Ref. 6-3). Representation of the 8.1-MeV monoenergetic source neutrons, as stated in the paper by M. H. Kalos (Ref. 6-1), cannot be easily accomplished with the above energy group cross-section set. To best simulate an 8.1-MeV neutron source, the neutrons were selected from energy group 4 (8.18 to 6.70 MeV). When the total cross section of this energy group was considered, the mean source neutron energy for the group was 7.3 MeV. The direction of the source neutrons had to be normally incident to the surface of the slab. Because of the discrete angular quadrature sets in ANISN, an approximation in the source initiated incident direction for a neutron source particle was made. Discrete cosine values of 0.9512 and 0.9805 were used in the S_8 and S_{16} calculations, respectively, which best simulate a monodirection neutron source normally incident to the slab of hydrogen.

Flux-to-dose conversion factors by energy group are listed in Table 6-1 for the single-collision neutron dose (rad/n· cm^2) and multiple-collision neutron dose (rad/n· cm^2)

6.2   RESULTS

The calculated ANISN fluxes and doses are tabulated in Table 6-2 for the slab of hydrogen from 5 to 100 mean free paths. Included in the table are the neutron fluxes (n/cm^2-sec) for both S_8 and S_{16} order of angular quadrature data and mesh spacing of approximately 0.125 to 1.0 mean free paths for various depths in the hydrogen slab. One mean free path of hydrogen in water is 12.5 centimeters for the energy interval of 8.18 to 6.70 MeV with an average energy of 7.3 MeV.

TABLE 6-1. NEUTRON ENERGY GROUP STRUCTURE FOR HYDROGEN IN H_2O PROBLEM

NEUTRON ENERGY GROUP (MeV)		SINGLE-COLLISION NEUTRON DOSE $(rad/N \cdot cm^2)$	MULTIPLE-COLLISION NEUTRON DOSE $(rad/N \cdot cm^2)$
14.9	to 12.2	5.46(-9)	7.0(-9)
12.2	to 10.0	5.13(-9)	7.0(-9)
10.0	to 8.187	4.84(-9)	7.08(-9)
8.187	to 6.703	4.62(-9)	6.88(-9)
6.703	to 5.488	4.53(-9)	6.23(-9)
5.488	to 4.493	4.70(-9)	5.73(-9)
4.493	to 3.679	4.11(-9)	5.15(-9)
3.679	to 3.012	4.00(-9)	4.76(-9)
3.012	to 2.466	3.30(-9)	4.49(-9)
2.466	to 2.019	3.14(-9)	4.20(-9)
2.019	to 1.653	3.00(-9)	4.13(-9)
1.653	to 1.353	2.69(-9)	4.00(-9)
1.353	to 1.108	2.51(-9)	3.89(-9)
1.108	to 9.072(-1)*	2.42(-9)	3.77(-9)
9.072(-1)	to 6.081(-1)	1.91(-9)	3.32(-9)
6.081(-1)	to 4.076(-1)	1.61(-9)	2.46(-9)
4.076(-1)	to 1.111(-1)	1.03(-9)	1.70(-9)
1.111(-1)	to 1.503(-2)	4.44(-10)	8.93(-10)
1.503(-2)	to 3.355(-3)	6.94(-11)	5.44(-10)
3.355(-3)	to 5.829(-4)	1.38(-12)	6.07(-10)
5.829(-4)	to 1.012(-4)		6.72(-10)
1.013(-4)	to 2.902(-5)		5.33(-10)
2.902(-5)	to 1.068(-5)		3.80(-10)
1.068(-5)	to 3.059(-6)		3.42(-10)
3.059(-6)	to 1.125(-6)		3.27(-10)
1.125(-6)	to 4.140(-7)		3.23(-10)
4.149(-7)	to Thermal		3.20(-10)

*Read as 1.108 to 9.027×10^{-1}

TABLE 6-2. NEUTRON FLUX AND DOSE AS A FUNCTION OF MEAN FREE PATHS AND DISTANCE

MEAN FREE PATH (MFP)	DISTANCE (cm)	S_8 0.125 MFP (n/cm²-sec)	S_8 0.500 MFP (n/cm²-sec)	S_{16} 0.500 MFP (n/cm²-sec)	S_{16} 0.250 MFP (n/cm²-sec)	S_8 0.250 MFP (n/cm²-sec)	S_{16} 1.0 MFP (n/cm²-sec)	UNCOLLIDED FLUX (n/cm²-sec)	SINGLE-COLLISION DOSE (rad/sec)	DOSE (rad/sec)
5	62.5	1.80(-01)*	2.00(-01)	2.20(-01)	2.00(-01)	1.50(-01)	2.25(-01)	6.74(-03)	1.38(-10)	2.50(-10)
10	125.0	1.72(-03)	1.90(-03)	2.20(-03)	2.00(-03)	2.00(-03)	3.35(-03)	4.54(-05)	1.07(-12)	2.00(-12)
15	187.5	1.35(-05)	1.406(-05)	1.78(-05)	1.50(-05)	1.35(-05)	3.40(-05)	3.06(-07)	7.40(-15)	1.50(-14)
20	250.0	9.23(-08)	1.00(-07)	1.40(-07)	1.40(-07)	9.40(-08)	3.10(-07)	2.06(-09)	4.50(-17)	9.10(-17)
25	312.5	6.53(-10)	6.2(-10)	9.5(-10)	9.22(-10)	6.50(-10)	2.85(-09)	1.39(-11)	2.75(-19)	5.50(-19)
30	375.0		3.30(-12)	4.75(-12)	7.20(-12)	4.20(-12)	2.20(-11)	9.36(-14)	1.65(-21)	3.30(-21)
35	437.5		1.97(-14)	4.03(-14)	5.11(-14)	2.87(-14)	2.00(-13)		1.02(-23)	1.99(-23)
40	500.0		1.30(-16)	2.50(-16)	3.40(-16)	1.75(-16)	1.50(-15)	4.25(-18)	6.00(-28)	1.21(-25)
45	562.5		8.80(-19)	1.80(-18)	2.40(-18)	1.30(-18)	9.0(-18)		3.60(-28)	7.40(-28)
50	625.0		4.79(-21)	8.23(-21)		8.00(-21)	8.0(-20)	1.93(-22)	2.09(-30)	4.30(-30)
60	750.0		1.85(-25)				5.0(-24)	8.75(-27)	8.00(-35)	1.60(-34)
70	875.0		6.75(-30)				2.71(-28)	3.97(-31)	3.00(-39)	6.18(-39)
80	1000.0		2.00(-34)				1.50(-32)	1.80(-35)	1.00(-43)	2.05(-43)
90	1125.0		9.00(-39)				1.10(-36)	8.19(-40)	3.70(-48)	7.60(-48)
100	1250.0		2.82(-43)				4.5(-41)	3.72(-44)	1.30(-52)	2.75(-52)

*READ AS 1.80×10^{-1}

Column 1 lists the mean free paths from 5 to 100. Column 2 gives the corresponding distance in centimeters. Columns 3 to 8 provide the neutron flux (n/cm^2-sec) for 0.125, 0.25, 0.5, and 1.0 mean free path mesh spacing for both S_8 and S_{16} order of angular quadrature values at various depths in the hydrogen slab. The neutron flux quantities for mesh spacing of 0.25 and 0.5 mean free path illustrate how these results converge to the smaller mesh value of 0.125 mean free path. For the larger mesh value of 1.0 mean free path, the neutron flux in Column 8 diverges from the flux in the smaller mesh. The uncollided neutron flux for a plane monodirectional source is listed in Column 9. For the mesh spacing of 0.5 mean free path and using an S_8 order of angular quadrature set, Columns 10 and 11 present the single-collision neutron dose and multiple-collision neutron dose (rad/sec), respectively. The results from Table 6-2 can be manipulated to determine the flux or dose buildup factors as a function of depth in centimeters or mean free paths. The resultant fluxes from these ANISN calculations required a maximum of 5 minutes of computer time (CPU) on the MSFC UNIVAC 1108. When this maximum time is compared to what would have been required by a Monte Carlo program (on the order of 30 to 60 minutes), it becomes apparent that the one-dimensional discrete ordinate solution is significantly faster than the Monte Carlo solution for this type of problem. It was shown that the results obtained when using the S_{16} angular quadrature data are slightly higher than those when S_8 was used. This conclusion is based on the fact that the cosine of the source neutron using S_{16} angular quadrature data approaches closer to the normal than the cosine in the S_8 angular quadrature data.

6.3   RECOMMENDATIONS AND CONCLUSIONS

The model development and approximations used in the solution of the slab of hydrogen were the best available within the limits of time and funding of the contract. A higher-order angular quadrature set, S_{32} or S_{64}, could be employed to better simulate the source which is normally incident to the surface of a slab. To better simulate a mono-energetic source, the energy group structure for the cross section data should be regrouped into a finer mesh, such as 8.2 to 8.0 MeV, which bounds the source energy of 8.1-MeV neutrons instead of the broad group 8.18 to 6.70 MeV, as used in this calculation. The MSFC UNIVAC 1108 computer storage presented some limitations to the hydrogen slab problem. Data for 100 mean free paths using 0.5 mean free path mesh intervals could be stored on the computer. However, the original problem was to include an equivalent distance of 200 mean free paths in hydrogen. A scheme that would allow for more than a total of 100 mean free paths has been devised in ANISN. A brief representation of of the techniques used is shown in Figure 6-3.

FIGURE 6-3.   SCHEME FOR DEEP PENETRATION USING ANISN WITH OVERLAPPING MESH INTERVALS

ANISN would be set up in the normal procedure using vacuum interfaces for PART I with small mesh spacing out to 25 mean free paths. A similar mesh spacing would be used for the hydrogen slab section in PART II which overlaps the mesh spacing described by PART I. The neutron flux determined in PART I at mesh spacing near the right boundary (4 to 6 mean free paths) would be used as the source data for PART II. The overlapping mesh interval that occurs in PART I and PART II is necessary to overcome the boundary and effect in the ANISN neutron flux results. Similarly, a continuation of this procedure up to 200 mean free paths in ANISN for significant distances is conceivable using one ANISN source deck or program file on tape and sequential data decks for each overlapping section. The availability of time and funding during this contract study did not permit the implementation of this technique. The discrete ordinate methods used in this study considered only the material of hydrogen in water. Other materials could be considered for deep penetration problems.

REFERENCES - SECTION 6

6-1.   Kalos, M. H., "Importance Sampling in Monte Carlo Shielding Calculations", Nuclear Science and Engineering 16, pp. 227-234, 1963

6-2.   Soltesz, R. G. and R. K. Disney, "One-Dimensional Discrete Ordinates Transport Technique", Volume 4, Report No. WANL-PR(LL)-034, June 1970

6-3.   Private communications with Juanita Wright, Radiation Shielding Information Center, Oak Ridge, Tennessee, June 1971